Invited Paper

Time-reversal and nonlocal effects in $\mathcal{PT}$-symmetric nonlinear lattices with balanced gain and loss

Andrey A. Sukhorukov[a], Zhiyong Xu[a], Sergey V. Dmitriev[b], Sergey V. Suchkov[b], and Yuri S. Kivshar[a]

[a] Nonlinear Physics Centre and Centre for Ultrahigh-bandwidth Devices for Optical Systems (CUDOS), Australian National University, Canberra, ACT 0200, Australia
[b] Institute for Metals Superplasticity Problems, Russian Academy of Science, Ufa 450001, Russia

ABSTRACT

We reveal a number of fundamentally important effects which underpin the key aspects of light propagation in photonic structures composed of coupled waveguides with loss and gain regions, which are designed as optical analogues of complex parity-time (or $\mathcal{PT}$) symmetric potentials. We identify a generic nature of time-reversals in $\mathcal{PT}$-symmetric optical couplers, which enables flexible control of all-optical switching and a realization of logic operations. We also show that light propagation in $\mathcal{PT}$-symmetric structures can exhibit strongly nonlocal sensitivity to topology of a photonic structure. These results suggest new possibilities for shaping optical beams and pulses compared to conservative structures.

Keywords: Parity-time symmetry, coupled waveguides, nonlinear optics

1. INTRODUCTION

Photonic structures composed of coupled waveguides with loss and gain regions offer new possibilities for shaping optical beams and pulses compared to conservative structures.[1–4] Such structures can be designed as optical analogues of complex parity-time (or $\mathcal{PT}$) symmetric potentials, which can have a real spectrum corresponding to the conservation of power for optical eigenmodes, however the beam dynamics can demonstrate unique features distinct from conservative systems due to nontrivial wave interference and phase transition effects,[5–10] offering new possibilities for all-optical beam control in the nonlinear regime[11–15] Most recently, $\mathcal{PT}$-symmetric properties in couplers composed of two waveguides have been demonstrated experimentally.[16,17]

In this work, we first overview in Sec. 2 our recent results[15] revealing a generic connection between the effect of time-reversals and nonlinear wave dynamics in systems with parity-time ($\mathcal{PT}$) symmetry. We consider a nonlinear optical coupler with balanced gain and loss, and show that for intensities below a threshold level, the amplitudes oscillate between the waveguides, and the effects of gain and loss are exactly compensated after each period due to periodic time-reversals. For intensities above a threshold level, nonlinearity suppresses periodic time-reversals leading to the symmetry breaking and a sharp beam switching to the waveguide with gain. Another nontrivial consequence of linear $\mathcal{PT}$-symmetry is that in the nonlinear regime, the threshold intensity remains the same when the input intensities at waveguides with loss and gain are exchanged. Then, in Sec. 3 we present our latest findings on the phenomenon of nonlocality in $\mathcal{PT}$-symmetric photonic lattices. Specifically, we reveal that nonlocality can lead to pronounced differences between optical beam dynamics in arrays of coupled waveguides with the same characteristics but different topology.

Further author information available at the Nonlinear Physics Centre web site: http://physics.anu.edu.au/nonlinear

Active Photonic Materials IV, edited by Ganapathi S. Subramania, Stavroula Foteinopoulou,
Proc. of SPIE Vol. 8095, 80950N · © 2011 SPIE · CCC code: 0277-786X/11/$18 · doi: 10.1117/12.894528

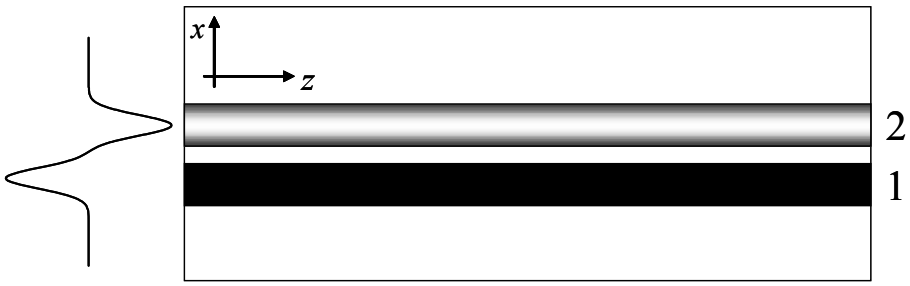

Figure 1. Scheme of nonlinear $\mathcal{PT}$-symmetric directional coupler with balanced loss in waveguide 1 and gain in waveguide 2. The arrow indicates the propagation direction (z).

2. TIME-REVERSALS IN $\mathcal{PT}$-SYMMETRIC NONLINEAR COUPLERS

It has been established already two decades ago that directional couplers with gain and loss[1] can offer benefits for all-optical switching in the nonlinear regime, lowering the switching power and attaining sharper switching transition. Recently, these conclusions were complimented by the prediction of unidirectional switching and exact analytical solution describing the switching dynamics in nonlinear $\mathcal{PT}$ symmetric couplers.[14] Here we overview the main results of our recent work,[15] demonstrating that although nonlinearity always breaks the $\mathcal{PT}$-symmetry conditions for asymmetric wave profiles even at arbitrarily small intensity levels, the effects of gain and loss are exactly compensated and $\mathcal{PT}$-symmetric dynamics is preserved *on average* due to periodic time-reversals, for intensities below a certain threshold. In contrast, for intensities above a threshold, nonlinear self-action suppresses time-reversals and $\mathcal{PT}$-symmetric dynamics is broken both locally and globally, resulting in the asymmetric wave localization in the region with gain. This conclusion is based on the symmetry analysis which is applicable to a broad class of nonlinear local responses, including in particular the cases of cubic (as considered in Refs.[1,14]) or saturable responses. This is important in view of possible experimental realizations of such couplers in different material systems with various nonlinear response characteristics. For example, linear $\mathcal{PT}$-symmetric couplers have been demonstrated based on $LiNbO_3$ platform,[17] and this material possesses photorefractive nonlinearity with saturable response.

We describe the propagation of waves in a $\mathcal{PT}$-symmetric optical coupler by the equations for the mode amplitudes at the first and second waveguides. We use a set of coupled-mode equations which include additional terms accounting for Kerr-type nonlinearity:[1,17]

$$i\frac{da_1}{dz} + i\rho a_1 + Ca_2 + G(|a_1|^2)a_1 = 0, \quad i\frac{da_2}{dz} - i\rho a_2 + Ca_1 + G(|a_2|^2)a_2 = 0, \tag{1}$$

where z is the propagation distance, a_1 and a_2 are the mode amplitudes, $\rho = \rho_1 = -\rho_2$ defines the rates of loss in the first waveguide and gain in the second waveguide, C is the coupling coefficient between the modes of two waveguides, and function G characterizes the nonlinear response. We assume with no loss of generality that $C > 0$, since for negative C it is possible to make the transformation $a_2 \to -a_2$ and $C \to -C$. We also consider the values of gain/loss coefficient below the linear $\mathcal{PT}$-symmetry breaking threshold,[17] $\rho < C$.

In order to analyze nonlinear dynamics, it is convenient to represent the mode amplitudes in the following form,

$$a_1 = \sqrt{I(z)}\cos[\theta(z)]\exp[+i\varphi(z)/2]\exp[i\beta(z)], \quad a_2 = \sqrt{I(z)}\sin[\theta(z)]\exp[-i\varphi(z)/2]\exp[i\beta(z)], \tag{2}$$

where I is the total intensity, θ and φ define the relative intensities and phases between the two input waveguides, and β is the overall phase. After substituting Eq. (2) into Eq. (1), we derive the closed system of evolution equations for I, θ, and φ:

$$\frac{dI}{dz} = -2\rho I\cos(2\theta), \quad \frac{d\theta}{dz} = \rho\sin(2\theta) - C\sin\varphi, \quad \frac{d\varphi}{dz} = G(I\cos^2\theta) - G(I\sin^2\theta) - 2C\cot(2\theta)\cos\varphi, \tag{3}$$

and additional equation for β:

$$\frac{d\beta}{dz} = \frac{1}{2}\left[G(I\cos^2\theta)/2 + G(I\sin^2\theta)\right] + \frac{C\cos\varphi}{\sin(2\theta)}. \tag{4}$$

In order to describe the features of nonstationary dynamics, we identify an important symmetry property of the model equations. After performing the complex conjugation of Eq. (1) and comparing it to the original equations, we conclude that for any solution $a_j(z)$,

$$\widetilde{a}_1(z_{0+}) = a_2^*(z_{0-})e^{i\delta},\ \widetilde{a}_2(z_{0+}) = a_1^*(z_{0-})e^{i\delta} \tag{5}$$

is also a solution of Eq. (1) for arbitrary constants z_0 and δ, where $z_{0\pm} = z_0 \pm z$. This transformation represents the action of $\mathcal{PT}$ operator, where parity operator ($\mathcal{P}$) corresponds to exchange of waveguide numbers and time operator ($\mathcal{T}$) defines the reversal of propagation direction. Using notations of Eq. (2), we express the transformation in Eq. (5) as

$$\widetilde{I}(z_{0+}) = I(z_{0-}), \quad \widetilde{\varphi}(z_{0+}) = \varphi(z_{0-}), \widetilde{\theta}(z_{0+}) = \pi/2 - \theta(z_{0-}), \quad \widetilde{\beta}(z_{0+}) = \delta - \beta(z_{0-}). \tag{6}$$

We notice that if $z_0 = z_m$ where

$$\theta(z_m) = \pi/4, \tag{7}$$

then we can choose the free parameter as $\delta = 2\beta(z_0)$, and solution transforms into itself at $z = z_m$. This happens because the intensity distribution is symmetric, $|a_1(z_m)|^2 \equiv |a_2(z_m)|^2$, and accordingly nonlinearity does not break the $\mathcal{PT}$-symmetry condition at $z = z_m$. Since the original and transformed solutions satisfy the same evolution equation, it follows that

$$\begin{aligned} &I(z_{m+}) = I(z_{m-}),\ \theta(z_{m+}) = \pi/2 - \theta(z_{m-}), \\ &\varphi(z_{m+}) = \varphi(z_{m-}),\ \beta(z_{m+}) = 2\beta(z_m) - \beta(z_{m-}), \end{aligned} \tag{8}$$

for $z_{m\pm} = z_m \pm z$ and any z_m which satisfies condition in Eq. (7). According to Eq. (8), the dynamics starting from z_m in positive ($+z$) and negative ($-z$) directions is exactly equivalent, subject to the effective exchange of waveguide numbers [Eq. (5)], and this is a nontrivial consequence of linear $\mathcal{PT}$ symmetry in the nonlinear regime. It also follows from Eqs. (3) and (7) that

$$\left.\frac{dI}{dz}\right|_{z=z_m} = 0. \tag{9}$$

The physical interpretation of this important result is that *the system exhibits effective time-reversal when the total intensity reaches the maximum or minimum values*, where time-reversal ($\mathcal{T}$) corresponds to change of the propagation direction (z). We use this result to reveal that for arbitrary nonlinear response functions, all solutions belong to two classes: (i) periodic solutions, where the intensities and relative phases in two waveguides are exactly restored after each period ($z \to z + z_p$), or (ii) solutions where the total intensity grows without bound due to nonlinearly-induced symmetry breaking. Let us prove that solutions are periodic if intensity is bounded, i.e. when there exists $z_{\max}$ where $dI/dz = 0$ and $d^2I/dz^2 < 0$ (we neglect the special case of a separatrix trajectory approaching a saddle point). Then, according to relation in Eq. (9), Eq. (8) should be satisfied simultaneously for $z_m = z_{\max}$ and $z_m = z_{\min}$, i.e.

$$I(z_{\min} - z) = I(z_{\min} + z),\ I(z_{\max} - z) = I(z_{\max} + z) \tag{10}$$

Making a variable transformation $z \to (z_{\min} - z)$ and $z \to (z_{\max} - z)$ in the first and second relations in Eq. (10) respectively, we obtain

$$I(z) = I(2z_{\min} - z),\ I(z) = I(2z_{\max} - z). \tag{11}$$

Applying the second relation in Eq. (11) recursively after the first one, we find that

$$I(z) = I(2z_{\max} - 2z_{\min} + z). \tag{12}$$

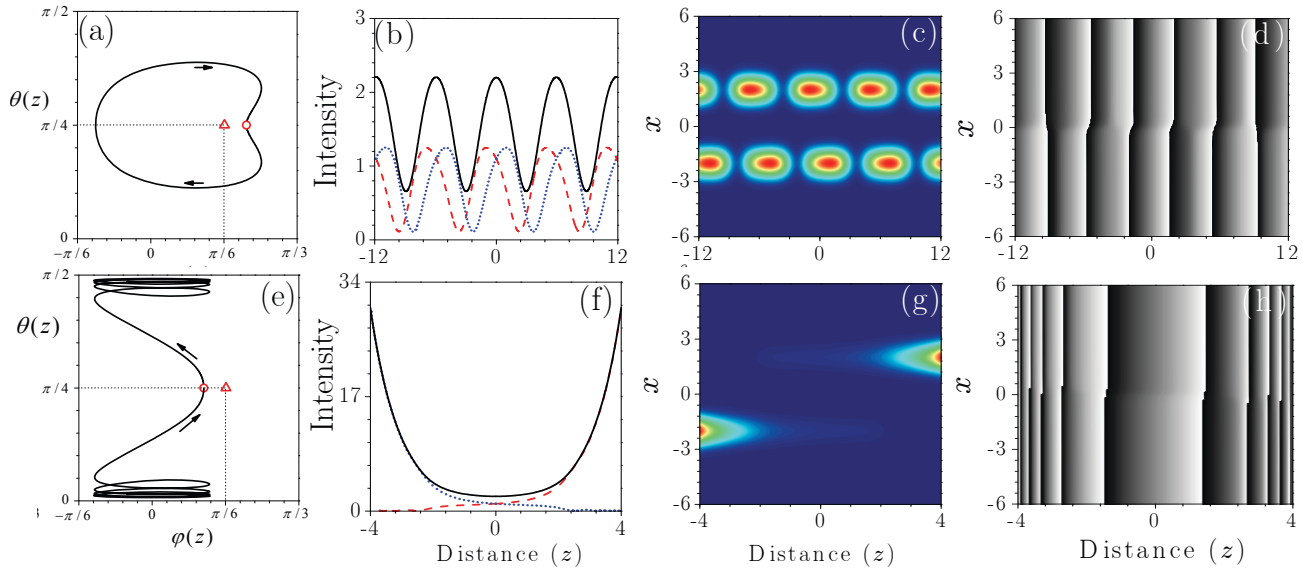

Figure 2. System dynamics for different initial conditions: (a)-(d) $\varphi = \pi/6 - \pi/20$ and (e)-(h) $\varphi = \pi/6 + \pi/20$. (a),(e) Trajectories in the phase plane (θ, φ). Red open circle marks the point at $z = 0$, and open triangle marks the unstable stationary solution with $\varphi_- = \pi/6$. (b),(f) Intensity dependencies on propagation distance in the first (dotted line) and second (dashed) waveguides, solid line show the sum of individual intensities. (c),(g) and (d),(h) show the intensity and phase evolution along the propagation direction. For all the plots, $\rho = 0.5$ and $I(z = 0) = 2.2$.

This means that the solution is periodic, with the period equal to $z_p = 2|z_{\max} - z_{\min}|$. This is a highly nontrivial result, since the model equation has three independent degrees of freedom (I, θ, ϕ), and such dynamical systems can in general exhibit quasi-periodic and chaotic behavior. It is a remarkable consequence of $\mathcal{PT}$-symmetry that dynamics can be only periodic or unbounded for arbitrary Kerr-type nonlinearities. We can determine the location of extrema points ($z_{\max}$ and $z_{\min}$) on the phase plane. It follows from Eq. (3) and (7) that maxima ($z_{\max}$) correspond to $\theta = \pi/4$ and $\varphi_- < \varphi < \varphi_+$, and minima ($z_{\min}$) to $\theta = \pi/4$ and $\varphi < \varphi_-$ or $\varphi > \varphi_+$.

Based on these general predictions, we can reveal a remarkable property. The type of nonlinear dynamics (periodic or unbounded) remains the same if we swap the intensities between the two waveguides [see Eq. (8)]. In particular, we can couple light at the input just to the first waveguide with loss, or to the second waveguide with gain, and the type of dynamics would be the same. This is a counter-intuitive result, since in the first case the total intensity will initially decrease, whereas in the second case the total intensity will be growing. However, in both cases the type of dynamics will be determined only by the initial intensity level. This is a highly nontrivial consequence of linear $\mathcal{PT}$-symmetry in the strongly nonlinear regime.

We complement the general analytical results with numerical examples. To be specific, we consider the Kerr-type nonlinear response function $G(I) = \gamma I$, where $\gamma > 0$ for self-focusing nonlinearity. Then, by introducing the transformation $z \to zC$ and $a_j \to a_j\sqrt{C/\gamma}$, we can scale the values of coefficients to unity, $C = 1$ and $\gamma = 1$, and we use these values in numerical simulations. We present in Fig. 2 two examples of system dynamics. In the first example presented in Fig. 2(a)-(d), the solution is periodic. We see that the trajectory in phase space rapidly moves away from the initial location, but then returns back after a full period. Completely different dynamics is observed in the second example [Fig. 2(e)-(h)], where the total intensity grows without bound and light becomes concentrated in a single waveguide at $|z| \to \infty$. These examples illustrate two generic types of the system dynamics.

3. NONLOCAL EFFECTS WITH $\mathcal{PT}$-SYMMETRIC DEFECTS

$\mathcal{PT}$-symmetric potentials appear in many physical contexts, and one feature actively investigated in the context of quantum theories is the property of *nonlocality*, where $\mathcal{PT}$-defect dynamics can be sensitive to potential profile at distant locations, and it was questioned the observability of such behavior in real physical systems.[18,19] In this

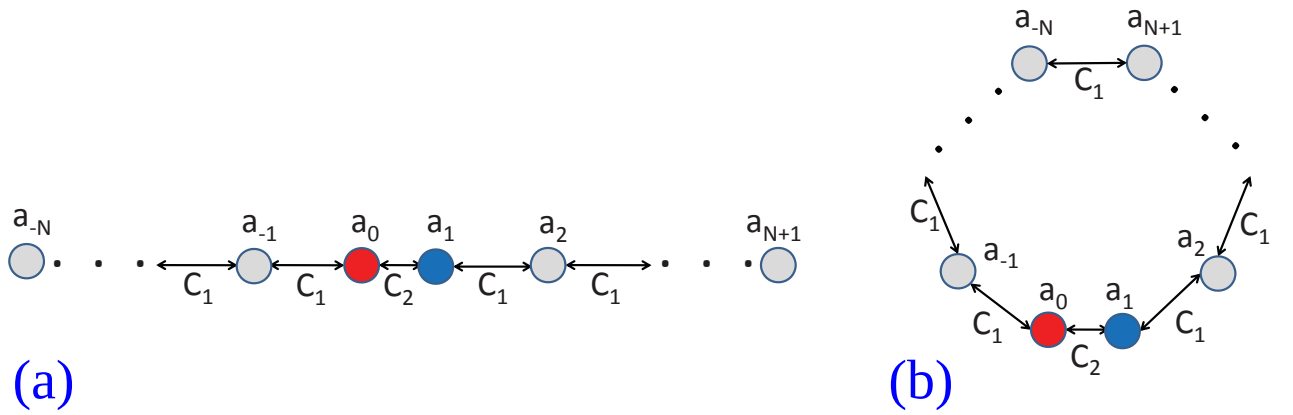

Figure 3. Schematic of a waveguide array with a pair of $\mathcal{PT}$-symmetric waveguides at sites $j = 0, 1$ with balanced gain and loss.

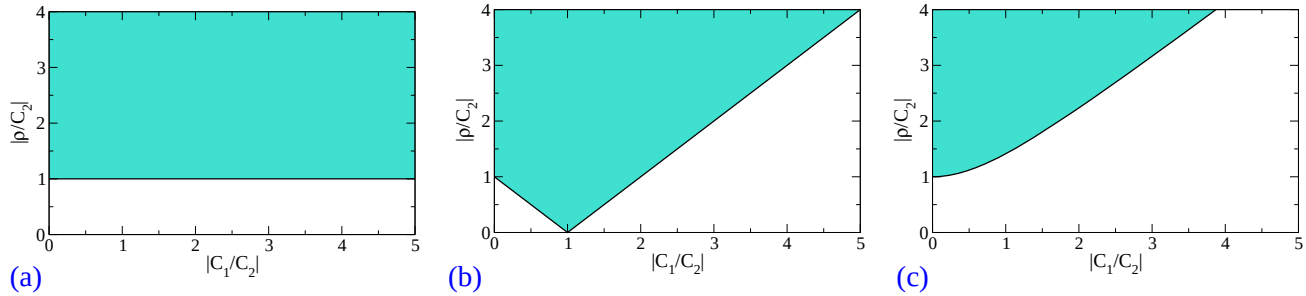

Figure 4. $\mathcal{PT}$ symmetry breaking regions shown with shading for (a) planar waveguide array, (b) circular waveguide array, and (c) infinitely long planar or circular waveguide array.

work, we reveal that effective nonlocality of $\mathcal{PT}$-symmetric structures with gain and loss elements can lead to pronounced differences for optical beam dynamics in arrays of coupled waveguides with the same characteristics but different topology.

To demonstrate the phenomenon of nonlocality in optical structures, we compare arrays of coupled optical waveguides with planar and circular geometries as schematically illustrated in Figs. 3(a) and (b), respectively. The beam profile is determined by the mode amplitudes a_j at individual waveguides, and mode overlap between waveguides is characterized by coupling coefficients: C_2 between the central waveguides $j = 0, 1$, and C_1 between all other neighboring waveguides. We consider $\mathcal{PT}$-symmetric structure composed of waveguide with gain at location $j = 0$ and with loss at the adjacent waveguide $j = 1$. The absolute magnitudes of gain/loss should be equal to satisfy $\mathcal{PT}$-symmetry condition. We use the coupled-model equations[10, 13, 17] to model the beam propagation:

$$i\frac{da_j}{dz} + C_1 a_{j-1} + C_1 a_{j+1} = 0, \; j \neq 0, 1, N+1, -N \tag{13}$$

$$i\frac{da_0}{dz} + i\rho a_0 + C_1 a_{-1} + C_2 a_1 = 0, \tag{14}$$

$$i\frac{da_1}{dz} - i\rho a_1 + C_2 a_0 + C_1 a_2 = 0, \tag{15}$$

where j is the waveguide number, z is the propagation distance, a_j are the mode amplitudes at waveguides, $\rho > 0 (< 0)$ defines the rate of loss (gain) at 0-th and gain (loss) at 1-st waveguides, and $C_{1,2}$ are the coupling coefficients between the modes of waveguides that can be tuned by changing the distance between the waveguides. The boundary conditions are zero for a planar structure [Fig. 3(a)],

$$a_{N+2} \equiv 0, \quad a_{-N-1} \equiv 0 \tag{16}$$

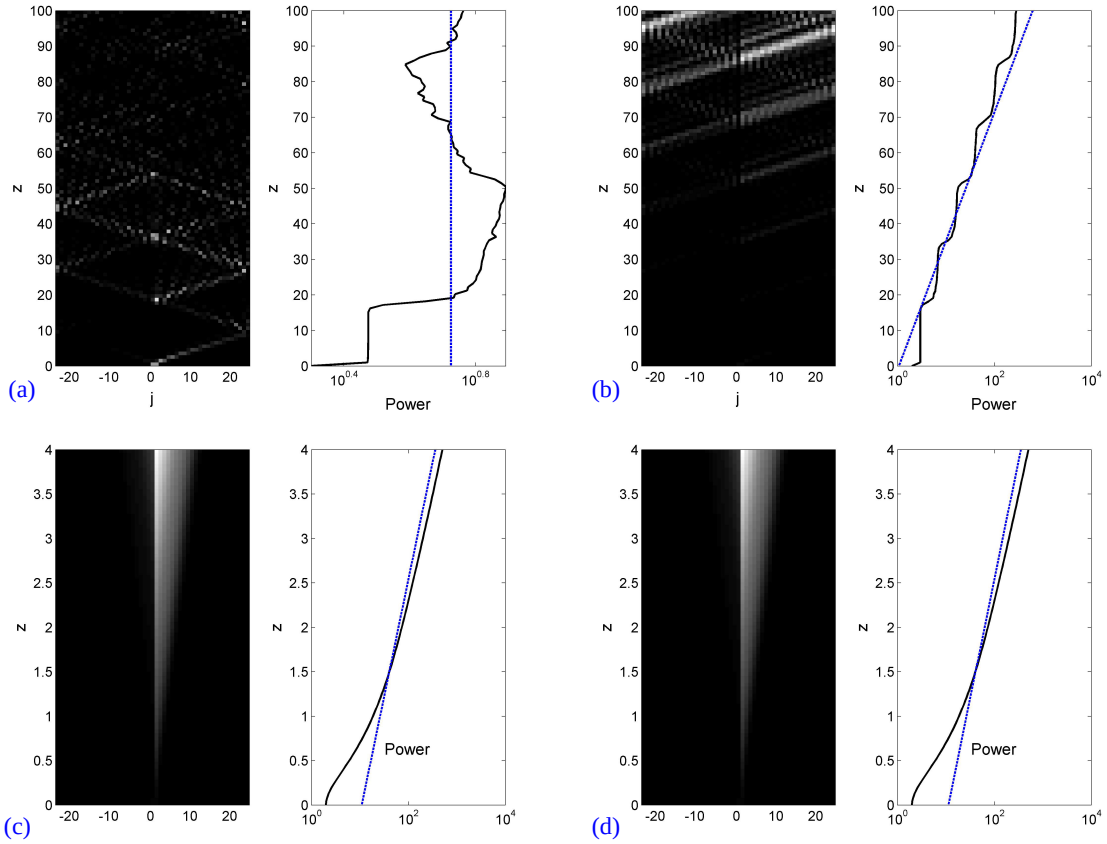

Figure 5. Optical beam dynamics in (a,c) planar and (b,d) circular waveguide arrays for (a,b) $\rho/C_2 = 0.8$ and (c,d) $\rho/C_2 = 2$. In each plot, left panel shows beam intensity profiles and right panel shows the calculated beam power (black solid line) and power trend for the most unstable eigenmode (dashed blue line) in logarithmic scale. For all the plots, $C_1/C_2 = 1.5$.

and periodic for a circular configuration [Fig. 3(b)],

$$a_{N+2} \equiv a_{-N}, \quad a_{-N-1} \equiv a_{N+1} \tag{17}$$

We note that Eqs. (13)-(15) are linear, since we consider the case of relatively weak optical intensities when the gain saturation and nonlinear effects can be neglected. Then, the beam dynamics can be described by representing the amplitude as a sum of eigenmodes, $a_j(z) = \sum_m B_m a_j^{(m)} \exp(i\lambda_m z)$. Here λ_m are the eigenvalues, $a_j^{(m)}$ are the eigenmode profiles, and B_m are the eigenmode excitation amplitudes determined by the input beam profile. A key feature of $\mathcal{PT}$-symmetric structures is that under certain conditions, the spectrum of all eigenmodes can be real (i.e. $\mathrm{Im}(\lambda_m) \equiv 0$), meaning that the effects of gain and loss can be compensated on average. On the contrary, if some of the eigenmodes have complex propagation constants, the mode amplitude can grow exponentially fast along the propagation direction as gain cannot be compensated by loss. For a $\mathcal{PT}$-symmetric coupler composed of two waveguides,[3, 16, 17] which can be modeled with Eqs. (13)-(15) by putting $C_1 = 0$, the spectrum is real when the value of gain/loss coefficient is below the threshold $|\rho| < |C_2|$. Considering the total number of waveguides N to be rather large but finite, we derive approximate analytical expressions for the thresholds in case of planar and circular array configurations. For a planar configuration, we find that the $\mathcal{PT}$-symmetry condition remains the same as for an isolated coupler, i.e. $|\rho| < |C_2|$, and somewhat surprisingly there is no dependence on the value of coupling coefficient in the rest of the array (C_1). This region is shown in Fig. 4(a). For a circular configuration, we determine that the threshold condition is modified and it now nontrivially depends on all the structure parameters, $||C_1| - |C_2|| \geq |\rho|$, and this region is plotted in Fig. 4(b). Most remarkably, the $\mathcal{PT}$ symmetry conditions separating fundamentally different cases of real spectrum, when the power is conserved

on average, and complex spectrum, when some guided modes experience amplification, are always different for planar and circular arrays of arbitrary size (N) – and this is a manifestation of nonlocality.

From a physical point of view, we should expect that if the structure size is increased towards infinity, the type of boundaries should not matter. We calculate the strongest growth rate characterized by $-\max_m \mathrm{Im}\lambda_m$ for different structure sizes and find that as $N \to \infty$, strong eigenmode amplification corresponding to $\mathcal{PT}$-symmetry breaking can occur only for the structure parameters corresponding to the region $\rho^2 > \rho_{\mathrm{cr}} = C_1^2 + C_2^2$, shown with shading in Fig. 4(c). When structural coefficients correspond to unshaded region in Fig. 4(c) (corresponding to $\rho < \rho_{\mathrm{cr}}$) but shaded region in Figs. 4(a) or (b), then there appear unstable modes however their growth rate reduces to zero as the structure size is increased. Accordingly, for a particular propagation distance, there will appear a structure size where the presence of slowly growing modes would be insignificant from a practical point of view.

We illustrate our predictions with numerical simulations. As an example, we consider the beam coupled to waveguide number $j = 1$ at the input, however similar scenarios are observed for other input conditions. We first choose the structure parameters $\rho/C_2 = 0.8$ and $C_1/C_2 = 1.5$ such that they correspond to stable regions for planar but unstable region for circular configuration, i.e. below the shaded area in Fig. 4(a) but inside the shaded area in Fig. 4(b). The plots of beam dynamics presented in Fig. 5(a) show that the power is conserved on average for planar structure. For the circular geometry, Fig. 5(b) demonstrates that power grows exponentially, and we also note that the power increases in "steps" since mode amplification occurs when wave is scattered on the central waveguides, and this happens periodically through beam circulation through the periodic boundary conditions. Such instability development would become slower as the structure size is increased and it would take longer for the wave to reach the boundaries and come back to the central region. This explains why such instabilities would disappear for infinitely large structures corresponding to unshaded region in Fig. 4(c). Completely different dynamics is observed for parameters $\rho/C_2 = 2$ and $C_1/C_2 = 1.5$, which fall within the shaded regions for all the plots in Figs. 4(a,b,c). In this case, Figs. 5(c) and (d) show that the instability develops in the central region and the power grows at a steady rate for both planar and circular geometries, with practically no effect of the boundaries

These results demonstrate that optical wave dynamics in $\mathcal{PT}$-symmetric structures with gain and loss elements can be strongly nonlocal, and can be critically affected by the structure topology. This resolves the fundamental questions on the observability of nonlocality effects raised in the context of quantum theories,[18,19] and also indicated new opportunities in designing active photonic structures.

4. CONCLUSIONS

We have identified and analyzed the effects of $\mathcal{PT}$-symmetry associated with optical nonlinearity and nonlocal sensitivity to distant boundaries in arrays of waveguides with a symmetric arrangement of gain and loss regions. We have revealed that in the nonlinear regime, time-reversals can support average balance between gain and loss despite nonlinearly-induced local $\mathcal{PT}$-symmetry breaking, whereas suppression of time-reversals at stronger nonlinearities results in switching and light concentration in a region with gain. We have also found that optical wave dynamics in $\mathcal{PT}$-symmetric structures with gain and loss elements can be critically affected by the structure topology due to effective nonlocality. Our results may offer a new insight and suggest different possibilities for optical beam shaping, switching, and amplification in linear and nonlinear photonic structures containing loss and gain elements.

This work was supported by the Australian Research Council through Centre of Excellence CUDOS, Fellowship, Discovery projects. SVD and SVS acknowledge financial support from the RFBR grant 11-08-97057-p_povolzhie_a.

REFERENCES

1. Y. J. Chen, A. W. Snyder, and D. N. Payne, "Twin core nonlinear couplers with gain and loss," IEEE J. Quantum Electron. **28,** 239–245 (1992).
2. A. Ruschhaupt, F. Delgado, and J. G. Muga, "Physical realization of PT-symmetric potential scattering in a planar slab waveguide," J. Phys. A **38,** L171–L176 (2005).

3. R. El-Ganainy, K. G. Makris, D. N. Christodoulides, and Z. H. Musslimani, "Theory of coupled optical PT-symmetric structures," Opt. Lett. **32,** 2632–2634 (2007).
4. S. Klaiman, U. Guenther, and N. Moiseyev, "Visualization of branch points in PT-symmetric waveguides," Phys. Rev. Lett. **101,** 080402–4 (2008).
5. K. G. Makris, R. El-Ganainy, D. N. Christodoulides, and Z. H. Musslimani, "Beam dynamics in PT symmetric optical lattices," Phys. Rev. Lett. **100,** 103904–4 (2008).
6. M. V. Berry, "Optical lattices with PT symmetry are not transparent," J. Phys. A **41,** 244007–7 (2008).
7. S. Longhi, "Bloch Oscillations in Complex Crystals with PT Symmetry," Phys. Rev. Lett. **103,** 123601–4 (2009).
8. S. Longhi, "Spectral singularities and Bragg scattering in complex crystals," Phys. Rev. A **81,** 022102–6 (2010).
9. K. G. Makris, R. El Ganainy, D. N. Christodoulides, and Z. H. Musslimani, "PT-symmetric optical lattices," Phys. Rev. A **81,** 063807–10 (2010).
10. M. C. Zheng, D. N. Christodoulides, R. Fleischmann, and T. Kottos, "PT optical lattices and universality in beam dynamics," Phys. Rev. A **82,** 010103–4 (2010).
11. Z. H. Musslimani, K. G. Makris, R. El-Ganainy, and D. N. Christodoulides, "Optical solitons in PT periodic potentials," Phys. Rev. Lett. **100,** 030402–4 (2008).
12. Z. H. Musslimani, K. G. Makris, R. El-Ganainy, and D. N. Christodoulides, "Analytical solutions to a class of nonlinear Schrodinger equations with PT-like potentials," J. Phys. A **41,** 244019–12 (2008).
13. S. V. Dmitriev, A. A. Sukhorukov, and Yu. S. Kivshar, "Binary parity-time-symmetric nonlinear lattices with balanced gain and loss," Opt. Lett. **35,** 2976–2978 (2010).
14. H. Ramezani, T. Kottos, R. El-Ganainy, and D. N. Christodoulides, "Unidirectional nonlinear PT-symmetric optical structures," Phys. Rev. A **82,** 043803–6 (2010).
15. A. A. Sukhorukov, Z. Y. Xu, and Yu. S. Kivshar, "Nonlinear suppression of time reversals in PT-symmetric optical couplers," Phys. Rev. A **82,** 043818–5 (2010).
16. A. Guo, G. J. Salamo, D. Duchesne, R. Morandotti, M. Volatier-Ravat, V. Aimez, G. A. Siviloglou, and D. N. Christodoulides, "Observation of PT-Symmetry Breaking in Complex Optical Potentials," Phys. Rev. Lett. **103,** 093902–4 (2009).
17. C. E. Ruter, K. G. Makris, R. El-Ganainy, D. N. Christodoulides, M. Segev, and D. Kip, "Observation of parity-time symmetry in optics," Nature Physics **6,** 192–195 (2010).
18. H. F. Jones, "Scattering from localized non-Hermitian potentials," Phys. Rev. D **76,** 125003–5 (2007).
19. M. Znojil, "Scattering theory using smeared non-Hermitian potentials," Phys. Rev. D **80,** 045009–12 (2009).